Published in IET Microwaves, Antennas & Propagation
Received on 18th October 2013
Accepted on 11th March 2014
doi: 10.1049/iet-map.2014.0117

ISSN 1751-8725

Meta-surfaces and antennas' radiation characteristics enhancement: planar microstrip and microstrip-based quasi-aperture antennas

Mahmoud Niroo-Jazi[1], Tayeb A. Denidni[2], Mohammad Reza Chaharmir[1,3], Abdel R. Sebak[1]

[1]*Department of Electrical and Computer Engineering, Concordia University, Montreal, Quebec, Canada H3G 1M8*
[2]*INRS, Université de Québec, Montreal, QC, Canada H5A1K6*
[3]*RF Technologies, Communications Research Centre Canada, 3701 Carling Avenue, P.O. Box 11490, Station H, Ottawa, ON, Canada K2H 8S2*
E-mail: m_nirooj@encs.concordia.ca

Abstract: Meta-surfaces as artificial magnetic conductors or high impedance surfaces to control the electromagnetic fields excited by a microstrip patch resonator are investigated for planar and non-planar structures. In the planar structure, two types of meta-surfaces are used as electromagnetic transducers to transform the captured non-radiating waves to radiated space waves, leading to about 4 dBi gain enhancement. Alternatively, by applying these surfaces as *E*-plane fences in two sides of a patch, a compact microstrip-based quasi-aperture antenna is proposed. The proposed antenna not only improves the gain up to 8 dBi, but also provides almost a symmetric radiation pattern by controlling the phase distribution of electric fields in the antenna aperture. Using near electric-field pattern inspection and characterising the meta-surfaces, the radiation mechanism of the proposed antennas are delineated. Two antenna prototypes are fabricated and tested and, confirming the simulated ones, the corresponding measured results are presented.

1 Introduction

Microstrip antennas have been one of the most interesting radiators in wireless communication systems for long time because of the wealth of advantages offered by the planar technology including, low profile, compatibility with printed circuits, fabrication simplicity and low cost [1, 2]. However, they naturally suffer from narrow bandwidth and low gain radiation characteristics [1, 3]. Typically, a microstrip antenna etched on a thin substrate offers a matching bandwidth and gain in the range of 3–5% and 5–7 dB, respectively. Therefore different creative techniques have been proposed to enhance its radiation characteristics, especially in terms of bandwidth and radiation pattern to meet the demands of the relevant communication systems [1, 3].

In the perspective of radiation pattern improvement, microstrip antennas have significantly evolved during the past two decades by taking benefits of the synergy between planar technologies with other innovative structures. For instance, by stacking one or two other patches on top of the resonator, the bandwidth and antenna directivity are enhanced [4–6]. In addition, patch antenna loaded with a superstrate or multilayer dielectric with periodically changed dielectric thickness and properties [called one-dimensional electromagnetic bandgap (1D-EBG) superstrate] have been developed to improve the antenna directivity by utilising the radiating leaky wave properties [7–9]. This technique has also been successfully applied for patch array configuration to improve directivity and matching bandwidth in [10].

Alternatively, corrugated metallic structures, also called soft surfaces, have been used to improve the antenna radiation pattern by controlling the propagating current on the ground plane [11, 12]. However, they are bulky and expensive, which this limits their applications in antennas. On the other hand, meta-surfaces have found significant interest for the purpose of antenna radiation pattern enhancement because of their unique electromagnetic responses to the incident/propagating waves that can be inexpensively realised with low-profile planar technologies [13–17]. Some of such meta-surfaces can be classified as EBG or high impedance surfaces (HISs), artificial magnetic conductors (AMCs) and partially reflective surfaces (PRSs) [18, 19]. As a meta-surface with partially reflective property, a periodic array of patches has been used to increase the antenna gain by imposing the principle of the Febry–Perot resonant cavity [20–22]. Furthermore, in [22], both properties of PRS and AMC have been combined together to considerably improve the antenna directivity, whereas its overall height has been reduced. In addition, in [23], the advantages of PEC and AMC are pulled together to obtain higher gain without losing the antenna efficiency. Alternatively, the properties of HIS or EBG structures have been used to enhance the radiation pattern of the microstrip patch antenna by suppressing the propagating surface waves [24] or creating a defect in the bandgap [25], respectively.

© The Institution of Engineering and Technology 2014

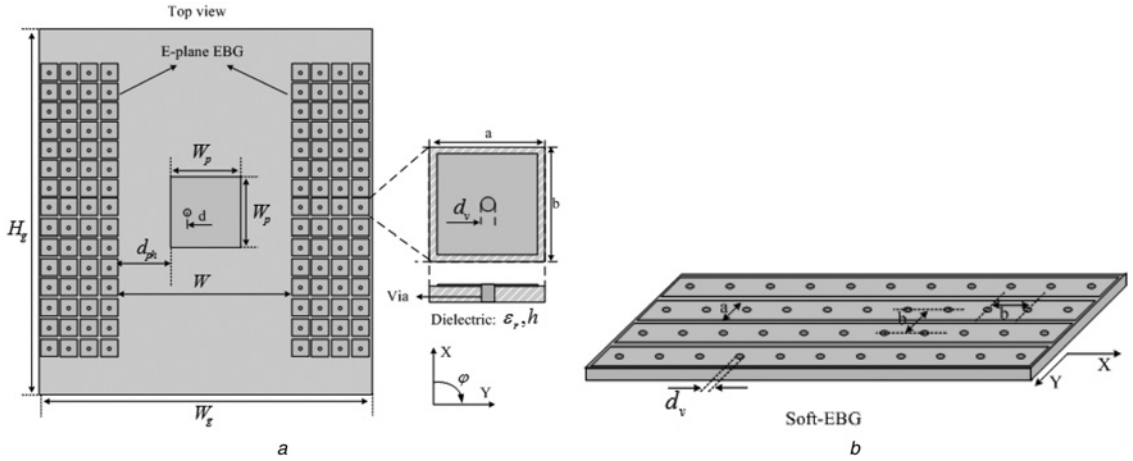

Fig. 1 *Geometry of the patch antenna surrounded by mushroom-like EBG and soft-EBG structures in the E-plane*

Antenna dimensions used in the simulations have been summarised in Table 1
a Patch antenna with mushroom-like EBG consisting of 4 × 15 unit cells
b Configuration of soft-EBG used instead of mushroom-EBG in Fig. 1*a*. The size of soft-EBG is equal to the one of mushroom-EBG

In this paper, not experimentally addressed so far, new trends of controlling the propagating electromagnetic waves in AMCs and HISs which enhance the radiation pattern performance of a patch antenna are presented. Indeed, the potentials of EBGs or HISs in capturing both the propagating surface- and coupled space-waves are explored in the planar configuration. Then, these captured waves with meta-surfaces are deliberately transformed to the radiated space waves, leading to a significant improvement in the antenna directivity. In the next step, the planar configuration is reformed to a non-planar structure to construct a microstrip-based quasi-aperture antenna (MBQAA). In this new compacted configuration, the advantages offered by soft-surfaces in aperture antennas [26–31] are mimicked by using the proposed meta-surfaces used in the *E*-plane of the patch antenna. The obtained results demonstrate that the directivity of patch antenna can be enhanced up to 8 dBi by controlling the electric field distribution in the aperture of the proposed MBQAA constructed with meta-surfaces. Furthermore, by using this configuration, the symmetry of antenna radiation pattern can be easily controlled as well.

2 Application of artificial materials in gain enhancement and the proposed antenna configurations

In this paper, artificial materials named meta-surfaces are used in planar and non-planar configurations. The antennas are designed to operate in the X-band at the centre frequency 9.4 GHz. In the first structure, meta-surfaces surround two sides of a coaxial-fed patch antenna in the *E*-plane; and entirely located on a same substrate, the antenna structure is planar. Although, referred as a non-planar configuration in the second case, they are used as *E*-plane fences for the planar microstrip patch antenna to create a compact MBQAA. This antenna offers a symmetric, high gain radiation pattern with a low cross-polarisation and low side/back lobe levels. It is light weight, cost effect and can be used as a feed for reflector antennas.

2.1 Meta-surfaces and gain enhancement in planar microstrip antennas

2.1.1 Design of the proposed planar antenna configuration: In Fig. 1*a*, mushroom-like EBG materials are used in the *E*-plane of a coaxial-fed microstrip patch antenna to improve its radiation performance by transforming surface waves to radiated ones, and hence enhancing the antenna gain by increasing its effective aperture efficiency. Furthermore, by eliminating the discontinuity of each EBG unit-cell along the *X*-direction, as shown in Fig. 1*b*, another type of HIS is created for the waves propagating in the *y*-direction. Indeed, this surface mimics the performance of a soft-corrugated surface [11, 12, 26–30], and therefore, named as soft-EBG structure, it is also used instead of the mushroom-EBGs applied in the *E*-plane of the antenna shown in Fig. 1*a*.

Four columns of mushroom-EBGs surround the two sides of the patch antenna in the *E*-plane at an appropriate distance from its radiating edges as shown in Fig. 1. The total number of unit cells in each column must be at least two times the patch width to effectively interact with the fringing fields of two resonant edges of the patch antenna.

Table 1 Final dimensions of simulated antennas

Antennas	ε_r	h	$W_p = L_p$	W_g	H_g	d	d_v	a	b	d_{ph}	W	h_c
simple patch	2.2	1.57	9.5	43.45	60	2.55	—	—	—	—	—	—
patch with planar *E*-plane EBG	2.2	1.57	9.5	44.5	60.5	1.57	0.36	2.8	2.95	10.225	26.95	—
patch with planar soft *E*-plane EBG	2.2	1.57	9.46	52.87	52.87	2.375	0.36	2.8	2.95	9.975	29.42	—
RQAA with metallica fence	2.2	1.57	9.405	43.45	60	2.9025	—	—	—	—	—	15.8
RQAA with mushroom-EBG fence	2.2	1.57	9.24	43.45	56.86	2.82	0.52	3.8	3.95	—		15.8
RQAA with soft-EBG fence	2.2	1.57	9.405	43.45	58.86	2.9025	0.52	3.8	3.95	—	—	15.8

© The Institution of Engineering and Technology 2014

doi: 10.1049/iet-map.2014.0117

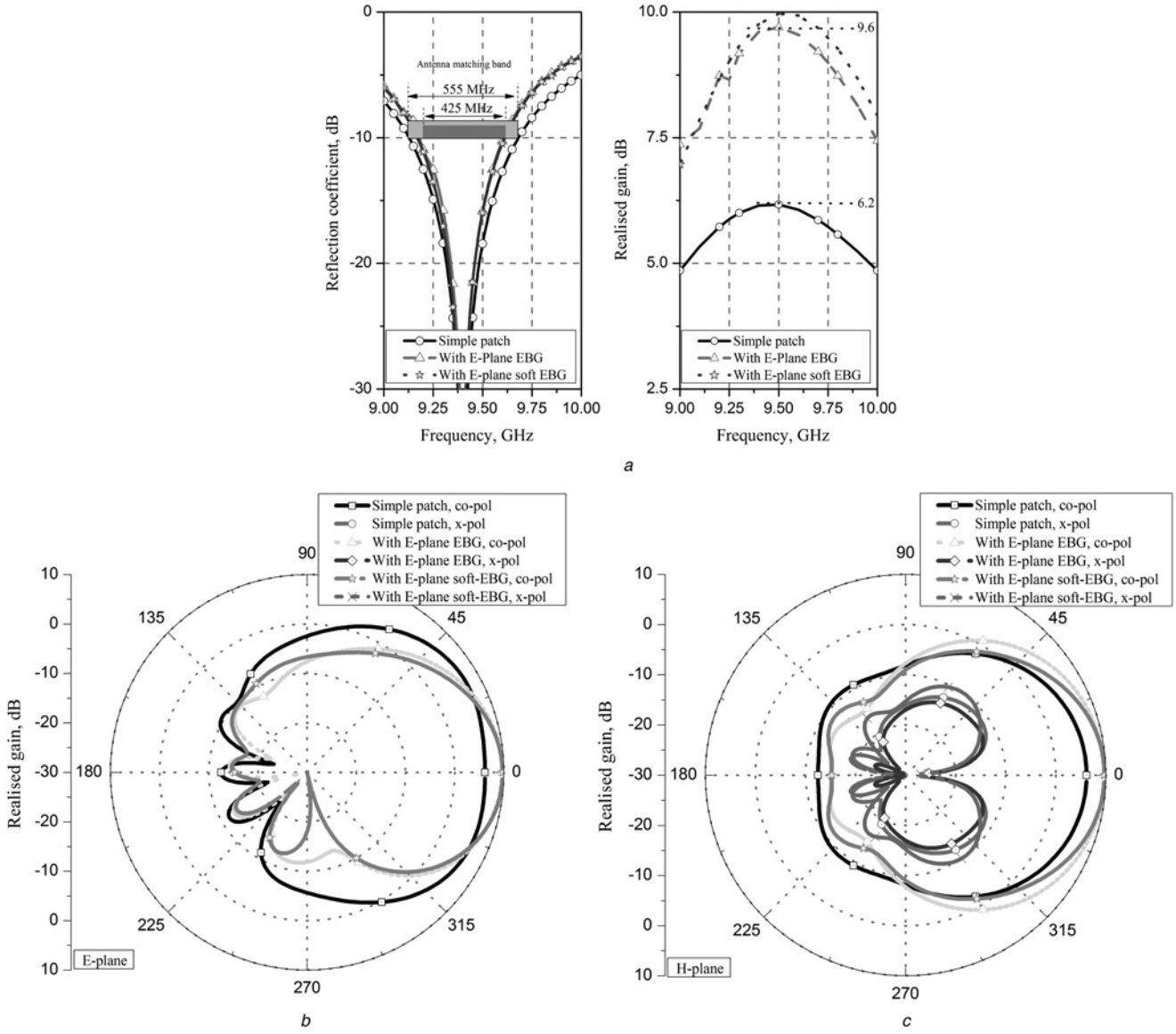

Fig. 2 *Simulated radiation characteristics of a simple patch antenna and the antennas described in Fig. 1*

Antenna dimensions have been summarised in Table 1
a Simulated reflection coefficients and realised gains
b *E*-plane radiation patterns
c *H*-plane radiation patterns

Table 2 Radiation characteristics of the RQAAs with metallic and meta-fences compared with a simple patch with and without artificial materials

Antenna/parameters	BW, MHz, sim/meas	Co-pol, sim/meas, dB		X-pol, sim/meas, dB		Beamwidth, °, sim/meas		Front to back ratio, dB, sim/meas	
		E (E_θ),	*H* (E_ϕ)	*E* (E_ϕ)	*H* (E_θ)	*E*	*H*	*E*	*H*
simple patch	555/–	7.1/–	6.2/–	–161/–	–18.6/–	100/–	60.5/–	–18.8/–	–15.3/–
patch with planar *E*-plane EBG	425/–	9.6/–	9.6/–	–164/–	–22.6/–	52.9/–	74	–20.6/–	–23.1/–
patch with planar soft *E*-plane EBG	440/–	9.8/–	9.8/–	–162/–	–20/–	46.4/–	81.8/–	–22.6/–	–21.4/–
RQAA with metallica fence	340/–	11/–	11/–	–160/–	–23/–	65.9/–	43.5/–	–21.5/–	–26.4/–
RQAA with mushroom-EBG fence	343/264	12.5/ 11.73	12.5/ –	–161/– 20.4	–24/– 20.665	36/35.8	45.3/ 35.6	–19.1/– 20.1	–26.2/– 26.8
RQAA with soft-EBG fence	327/305	13.1/ 12.2	13.1/ –	–174/– 17.84	–20.7/– 19.584	39.4/ 33.2	44.5/36	–26.1/– 18.9	–36.7/–25

Note: the results presented for the cases with mushroom-EBG and soft-EBG fences are related to the simulations, where compromises between back/side lobe, beam symmetry and maximum gain have been considered. The maximum gain of antennas for those cases can be enhanced by more than 1.5 dB by neglecting these compromises.

© The Institution of Engineering and Technology 2014

Therefore 15 unit cells are used for each column. Furthermore, to obtain the maximum constructive radiation out of the captured field by the EBGs in both sides of the patch, four columns of unit cells are enough, as it will be explained in the next sub-sections.

The initial sizes of the unit-cell are calculated using its equivalent resonant LC transmission line model [16]. In this model, the inductance represents the current passing through the via and the capacitance results from the coupling between fringing fields of adjacent patches. The values of inductance and capacitance are related to the unit-cell dimensions by expressions (1) and (2), and the resonant frequency of EBG is calculated by (3) [16]

$$L = \mu_0 h \tag{1}$$

$$C = \frac{a\varepsilon_0(1+\varepsilon_r)}{\pi} \cos h^{-1}\left(\frac{a+b}{b-a}\right) \tag{2}$$

$$\omega = \frac{1}{\sqrt{LC}} \tag{3}$$

Therefore the unit cells are designed to create a bandgap close to the desired operating frequency. Then to achieve the maximum realised gain and best matching performance, the antenna dimensions are optimised using CST Microwave Studio simulator. The crucial parameters used in the optimisation are a, b, W_p, d and d_p. The final dimensions of antennas are summarised in Table 1 for each case.

The radiation characteristics of the patch antenna integrated with meta-surfaces, that is, with mushroom-EBGs and soft-EBGs, were simulated and compared with a simple patch antenna with the same physical aperture area. These characteristics are demonstrated in Fig. 2 and they have been concisely summarised in Table 2. As it can be noted from the data in this table, both types of meta-surfaces reduce the matching bandwidth by almost 23%. Considering the distance between the radiating edges of the patch and EBGs, which is $0.31\lambda_0$, where λ_0 is the free space wavelength, this is mainly because of the indirect interactions between meta-surfaces and the microstrip patch antenna. These interactions are realised through the coupling mechanism between the patch and meta-surfaces because of the propagating surface waves and radiated space waves. The simulated gains of the antennas in Fig. 2*a* show that the meta-surfaces enhance the gain by 3.8 dB. The maximum value is obtained for the one surrounded with soft-EBG. Indeed, this is equivalent to about 14% aperture efficiency enhancement, that is, from 15.9 to 29.7%. It needs to highlight that, being out of the scale of

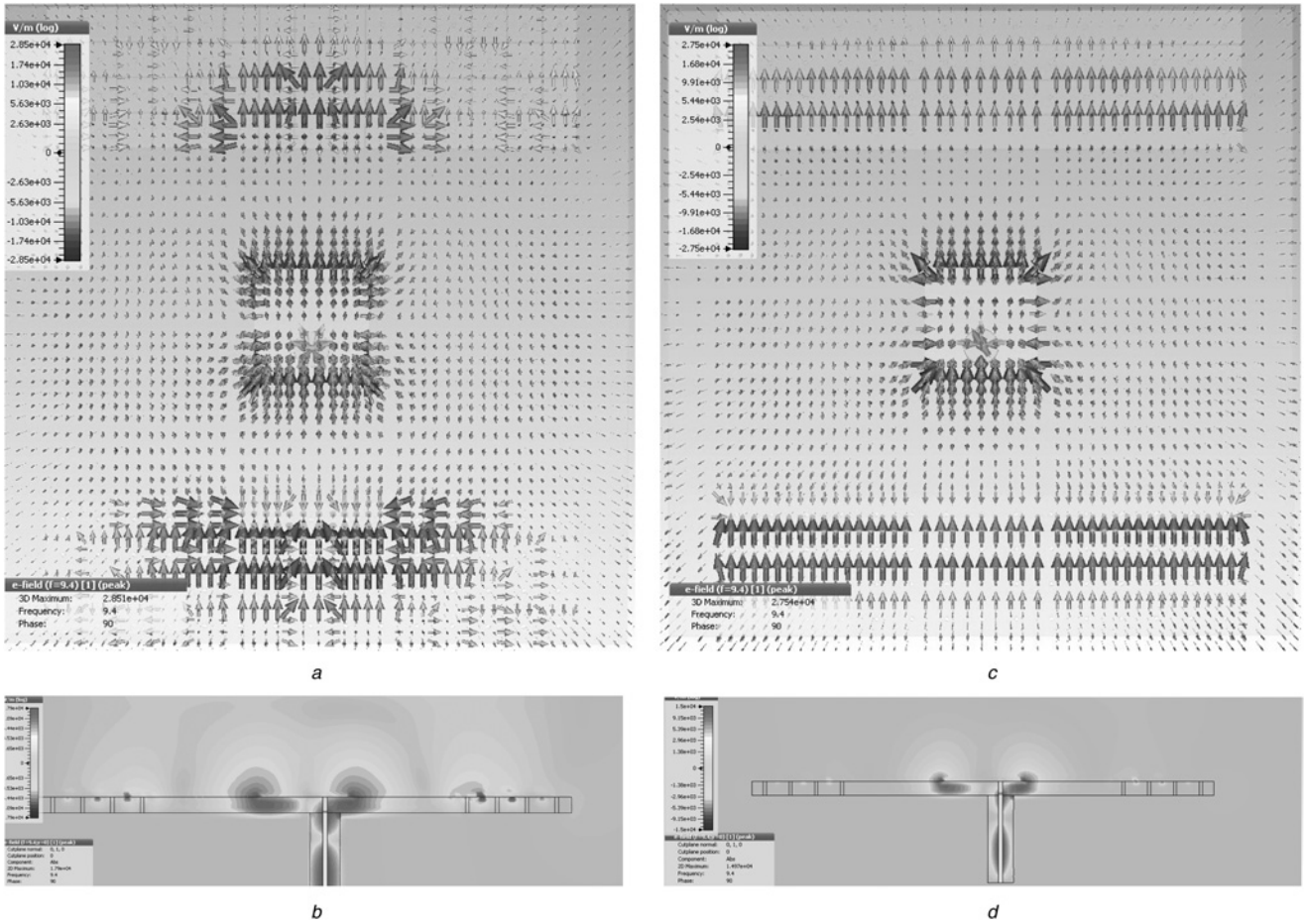

Fig. 3 *Near field examination of the proposed configurations shown in Fig. 1 at 9.4 GHz, that is, for the cases with E-plane mushroom-EBG (a and b) and with E-plane soft-EBG (c and d)*

Coordinates are referenced to the antenna configuration shown in Fig. 1
a Top view (*XY*-plane)
b Side view (*XZ*-plane)
c Top view (*XY*-plane)
d Side view (*XZ*-plane)

© The Institution of Engineering and Technology 2014

doi: 10.1049/iet-map.2014.0117

the figure, the cross-polarisation of antennas in *E*-plane patterns in Fig. 2*b* are missed in the figure.

2.1.2 Radiation mechanism of the proposed planar configuration: To further understand the principle behind the gain enhancement in these antennas, their near electric-field patterns at the centre frequency of the obtained matched bandwidth are examined. These patterns are illustrated in Fig. 3. The patterns in the *XY*-plane show that the meta-surfaces are significantly radiating in-phase with the radiation from edges of the microstrip patch antenna. In fact, the distance of EBGs from the edge of patch (d_{ph}) and the number of columns dictate the maximum realisable gain for this configuration. In other words, as the near electric-field patterns in the *XY* and *XZ* planes are also reflecting, the meta-surfaces increase the aperture efficiency of the patch antenna. It means that the total structure can be considered as an array of two patches, each one has a gain of about 7 dB, which are separated by a distance of less than λ_g (wavelength in the dielectric). These patterns also demonstrate that when patch is surrounded by the soft-EBG, the antenna aperture more effectively increases by suppressing the anti-phased radiating TE-wave and hence uniformly distributing the electric fields across the physical aperture area. This, indeed, leads to a better gain for the antenna surrounded by this type of meta-surface.

To identify the nature of the radiation from the EBG meta-surface which is contributing to the gain enhancement, the $K-\beta$ dispersion diagram of a unit-cell of the mushroom-EBG has been calculated using CST Microwave Studio for the first TE- and TM-modes propagating in three directions of its irreducible Brillouin zone as shown in Fig. 4*a*. The one of soft-EBG has also been determined for the propagation only in the *y*-direction, which is exhibited in Fig. 4*b*. In these figures, the propagating modes in the free space and an environment entirely filled with a dielectric material with permittivity equal to the one of EBG substrate are exhibited as references. The result for the mushroom-EBG surface demonstrates that the meta-structure operates as a hard-surface for the TE wave in the frequency range of 9–10 GHz, while it starts to suppress the TM wave from 9.7 GHz. This suppressing band is very close to the operating frequency of the patch antenna.

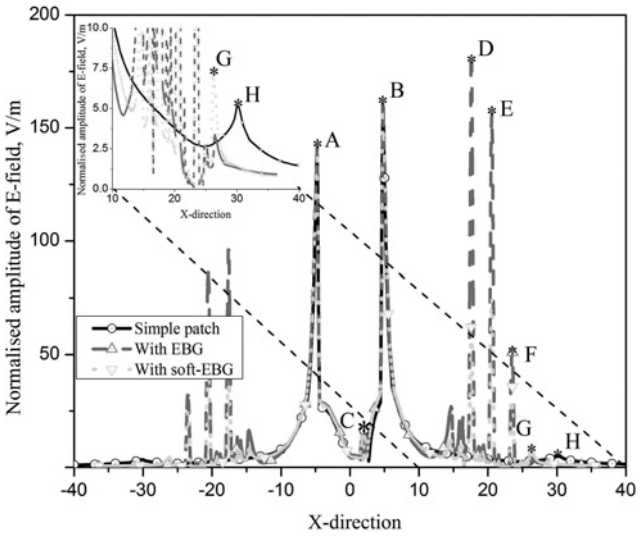

Fig. 5 *Normalised amplitudes of the electric-field distributions along the X-direction on the surface of the dielectric of patch antennas with/out meta-surfaces*

However, in the frequency range from 9.2 to 9.7 GHz, the TM propagating wave interacts with meta-surfaces, and then, it is transformed into the radiated leaky waves. This is in agreement with the work reported in [31], where only theoretically has proved the potential of such surfaces in supporting radiated leaky waves. Not shown here for brevity, our investigation shows that when the bandgap region of meta-surfaces are adjusted to cover the desired operating frequency range centred around 9.4 GHz just similar to the other works reported in [9–12], the gain enhancement is at least 1 dB less than the cases presented here.

Therefore it can be concluded that as a more effective HISs in two sides of the patch, these meta-surfaces interact with both the propagating surface waves on the dielectric/air interface and the radiated space waves by the patch antenna. Indeed, the electric fields captured by these surfaces in two sides of the patch transformed to the radiated space waves which are leaked out through the discontinuities between the EBG unit cells. Consequently, by appropriately

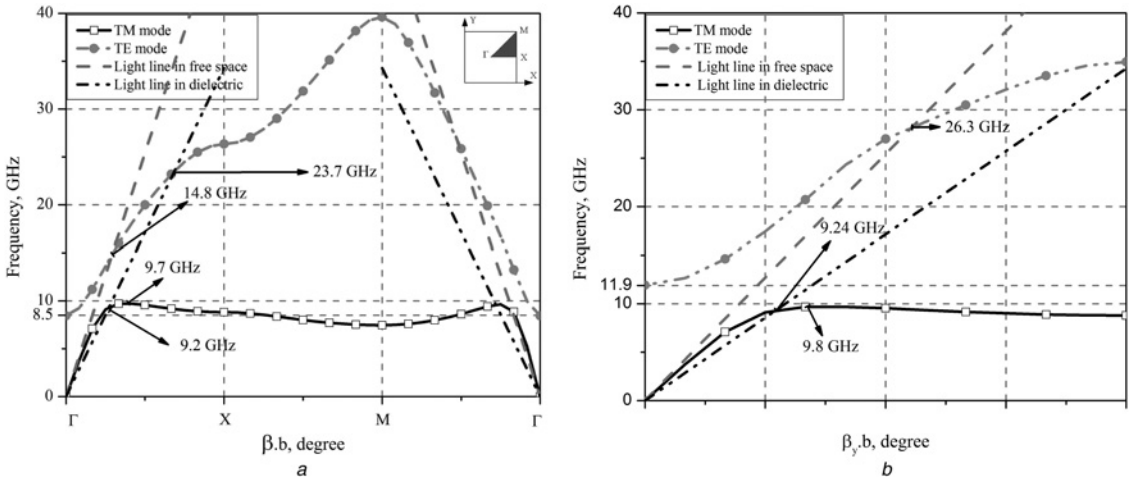

Fig. 4 *Simulated dispersion diagrams of EBG surfaces*

a Mushroom-EBG
b Soft-EBG

© The Institution of Engineering and Technology 2014

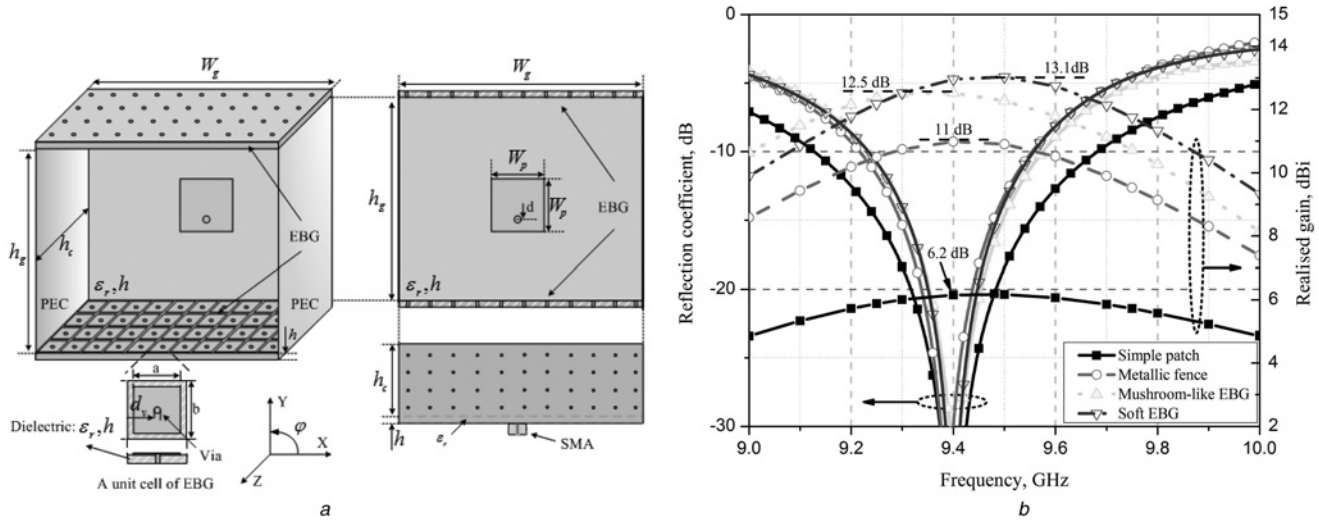

Fig. 6 *Reflection coefficient of the RQAAs compared with a simple patch and a patch with metallic fences*

Dimensions of simulated antennas have been summarised in Table 1
a Geometry of the proposed RQAA with meta-fences
b Simulated reflection coefficients and realised gains

adjusting the distance between radiating edges of the patch with these surfaces and the sizes of EBGs, these transformed radiated waves are constructively contributed in gain enhancement. This in fact is the main technical difference between the work presented here in which leaky waves are propagated through the meta-surfaces and the ones reported in [17, 22–24], where meta-surfaces are operating in their bandgap region and hence suppressing surface waves.

To more carefully examine this issue, the electric-field distributions on the dielectric surface along the *X*-direction (e.g. symmetric plane of the antenna passing through the feed point) are depicted for three cases in Fig. 5. The peaks in these curves indicate the level of electric field at each location. The curve calculated for simple patch demonstrates three peaks at locations named A, B and H, which are related to the radiating edges of the patch and scattered field from the substrate edge. The small peak at C is related to the feed point. Owing to the asymmetry in the *E*-plane, the level of the field at radiating edge B is higher than the one at A. By integrating meta-surfaces with patch antenna some more local maximums are appeared in the curves at D, E, F and G. This again confirms that the electric fields are captured by meta-surfaces and then they are transformed to the radiated leaky waves. In addition, since these fields are transformed to the radiated waves, the peak related to the scattered field at the substrate edge, that is, H location, is disappeared. As another interesting point, considering the level of the scattered field at H point and appearing such high peak levels at D, E and F locations, it is believed that the amount of improvement on the gain is not only because of transforming the surface wave to the radiated one. It is also related to the coupling between EBG-structures and the radiated space waves from edges of the patch. It is also worth to mention that because of the local field concentration around the *X*-axis, the level of the peak at D for the case with EBG meta-surfaces is much higher than the antenna integrated with soft-EBG.

For brevity, not demonstrated here, the simulation shows that minimum three rows of mushroom-EBG on each side of the patch antenna are enough to add at least 3 dB to the antenna gain, and by increasing the number of rows to more than six, it will not notably enhance the gain level beyond 9.9. In addition, when vias of mushroom-EBGs in Fig. 1*a* are eliminated, the antenna gain reduces to 5.4 dB in the *H*-plane, which is even less than the one of simple patch antenna. In this case, the meta-surfaces without vias conveniently support surface waves that cause to a significantly broadened radiation pattern, more notably in the *H*-plane (104 and 77° in *E* and *H* planes, respectively), and hence this leads to more radiation leakage from the substrate edges (–15.5 and –14.7 dB in *E* and *H* planes, respectively). Consequently, vias are the essential part of meta-surfaces in capturing the electric field and transforming them to the radiated waves.

The dispersion diagram calculated for the soft-EBG surface in Fig. 4*b* demonstrates a same performance for the TM surface wave with a slight change to the lower and upper edges of its bandgap. However, this meta-surface operates as a soft-EBG for the TE-waves across the entire 9–10 GHz frequency band, and therefore suppresses the electric-field component oriented along the *X*-direction. Consequently, for this case, leaked electric fields are more uniformly distributed along the *X*-direction. This leads to a slightly larger effective aperture area and hence a little gain improvement compared with the case with mushroom-EBGs.

Table 3 Aperture efficiency of the proposed antennas

Antennas	Physical area A (λ_0^2)	Aperture efficiencies, %	
		Sim.	Meas.
simple patch	2.562	15.9	—
patch with planar *E*-plane EBG	2.75	28.3	—
patch with planar soft *E*-plane EBG	2.75	29.7	—
RQAA with metallica fence	2.562	36.4	—
RQAA with mushroom-EBG fence	2.562	51.5	37.3
RQAA with soft-EBG fence	2.562	59.15	48

© The Institution of Engineering and Technology 2014

doi: 10.1049/iet-map.2014.0117

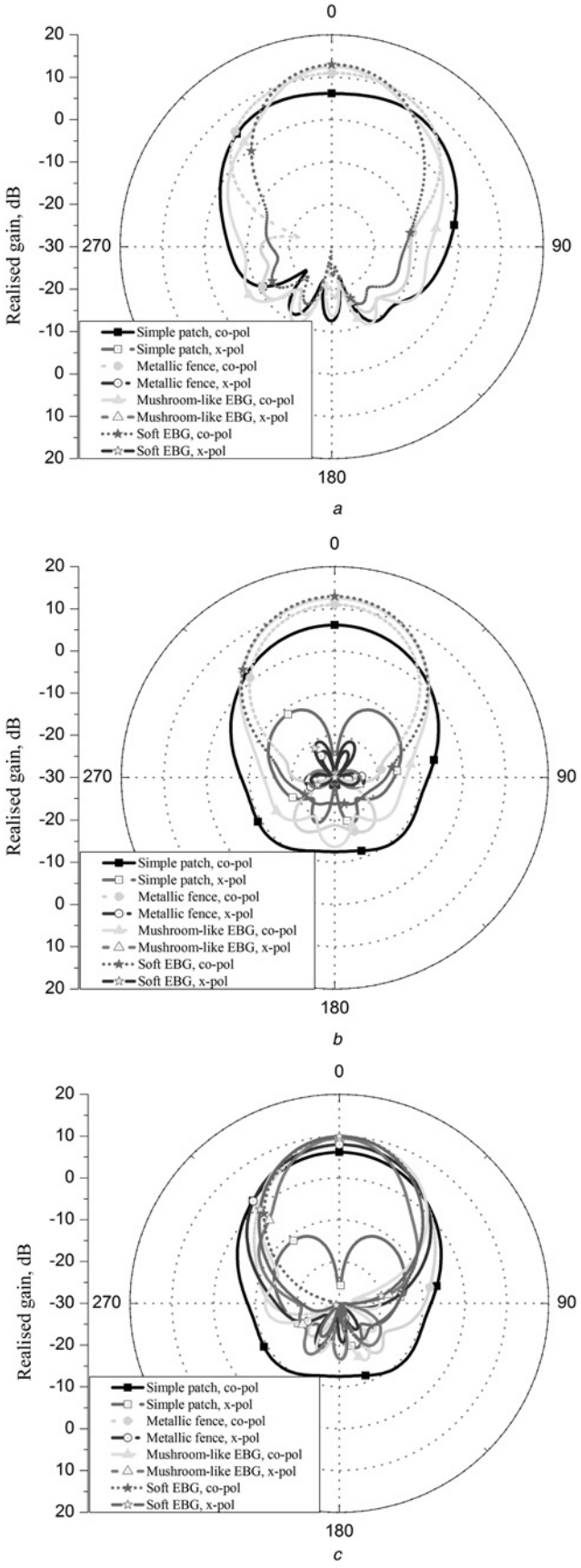

Fig. 7 *Radiation patterns of the RQAAs made with metallic and meta-fences*

a *E*-plane radiation pattern
b *H*-plane radiation pattern
c Radiation pattern at plane $\varphi = 45°$

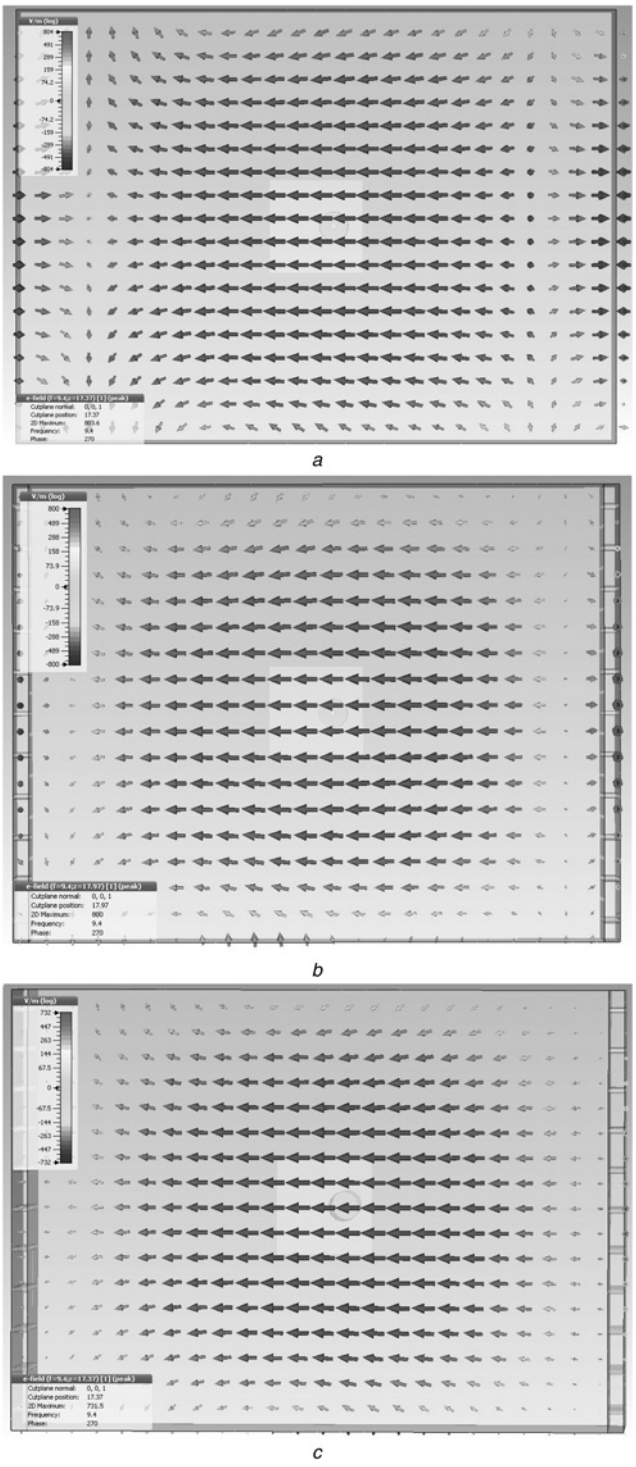

Fig. 8 *Aperture field distributions of the RQAAs made with metallic and meta-fences*

a Metallic fences
b Mushroom-like EBG fences
c Soft-EBG fences

The slight cross-polarisation enhancement of the antenna with soft-EBG is mainly because of the TE wave suppression, whereas for the antenna with mushroom-EBG is essentially because of the destructive radiation of cross-polarised field across the discontinuities in the *X*-direction as shown by the field distribution in Fig. 3*a*. The radiation characteristics of the antennas are summarised in Table 2.

© The Institution of Engineering and Technology 2014

2.2 Meta-surfaces and rectangular-quasi-aperture antenna

2.2.1 Design of the proposed non-planar antenna configuration: In this section, the proposed antenna configuration in Fig. 1 is modified to further enhance its performance in terms of gain and radiation pattern by taking advantages of the aperture antenna radiation mechanism. By folding the meta-surfaces of the antenna configuration shown in Fig. 1 and using two metallic fences in the *H*-plane, a rectangular-quasi-aperture antenna (RQAA) is introduced as depicted in Fig. 6*a*. Both mushroom-EBG and soft-EBG can be used as meta-fences in the *E*-plane of the proposed antenna. In this antenna, the number of unit cells is reduced to 11. Indeed, this results in a desired symmetric radiation pattern. Then, the dimensions of the patch antenna, EBGs and H_g are optimised using CST Microwave Studio in terms of matching, maximum gain and symmetric radiation pattern in both *E* and *H* planes with minimum back/side lob level. The final dimensions of antennas have been summarised in Table 1.

The simulated reflection coefficients and realised gains of RQAAs constructed with both mushroom- and soft-EBGs are compared in Fig. 6*b* to those of the simple patch antenna designed in the previous section. Furthermore, the performances of RQAA, when it is constructed with only metallic fences in both *E* and *H* planes, are also examined for more clarification. The height of metallic walls is as high as the RQAA with meta-surfaces.

Similar to the planar prototype discussed earlier, by using either metallic or meta-surfaces as fences in the *E*-plane of the patch antenna, the matching bandwidth is reduced almost by 40%. Nonetheless, the matching bandwidths of RQAAs constructed with meta-surfaces are almost similar to the one made with only metallic fence on its four sides. Furthermore, when meta-surfaces are used, the antenna configuration provides a high gain value of about 13.1 dB. This means that, having even smaller physical aperture area, RQAA composed of meta-surfaces increases the gain of simple patch antenna by about 7 dBi. In fact, by applying meta-surfaces as *E*-plane fences, the radiation principle of the structure more looks like the one of a rectangular aperture antenna. However, its performances are much better than the one with metallic fences, that is, the quasi-waveguide aperture antenna constructed with metallic walls. In addition, the simulation results show that by changing the patch sizes of EBG unit cells, the antenna gain can be increased to more than 14 dBi. However, in this case, some asymmetry is appeared in the *E*-plane radiation pattern. This is because the surface impedances of meta-surfaces on two sides of the patch antenna more constructively affect the waves propagating on its surface, leading to higher gain value. It needs to be highlighted that the total height of RQAA is $\lambda_0/2$ for both cases comprised of either mushroom-EBG or soft-EBG. This demonstrates that the proposed RQAAs are more compact compared with a metallic pyramidal horn with similar radiation performance. In addition, as summarised in Table 3, the total aperture efficiencies of these antennas are slightly better than the one of an optimal pyramidal horn antenna, which is about 50% [32].

For more clarification, the 45°, *E* and *H* planes radiation patterns of the antennas are compared with each other in Fig. 7. As it is obvious, the antennas with meta-surfaces provide narrower and more symmetric beams compared with the other two cases. In addition, the RQAA with the soft-EBG predicts the minimum back/side lobe level in all radiation planes. Being better than the simple patch, by using either metallic or meta-fence around the patch antenna, the cross-polarisation level is improved. It needs to be noted that because of the low level of cross-polarisation components in the *E*-plane radiation pattern, the cross-polarisation components are not in the scale range of the plot shown in Fig. 7*a*, and hence they are missed in this figure. The final simulated radiation characteristics of the antennas are summarised in Table 2.

2.2.2 Radiation mechanism of the proposed non-planar configuration: To investigate the effect of meta-surfaces on the antenna gain enhancement, the electric-field distributions in the aperture of the RQAAs constructed with meta-surfaces and metallic walls are compared with each other as shown in Fig. 8. It is clear that when meta-surfaces are used in the RQAA, the antiphase parts of the field distribution next to the side *E*-plane walls are considerably weakened for the antenna composed of mushroom-EBG, whereas those are almost vanished for the one with soft-EBG. That is why a more uniform field is

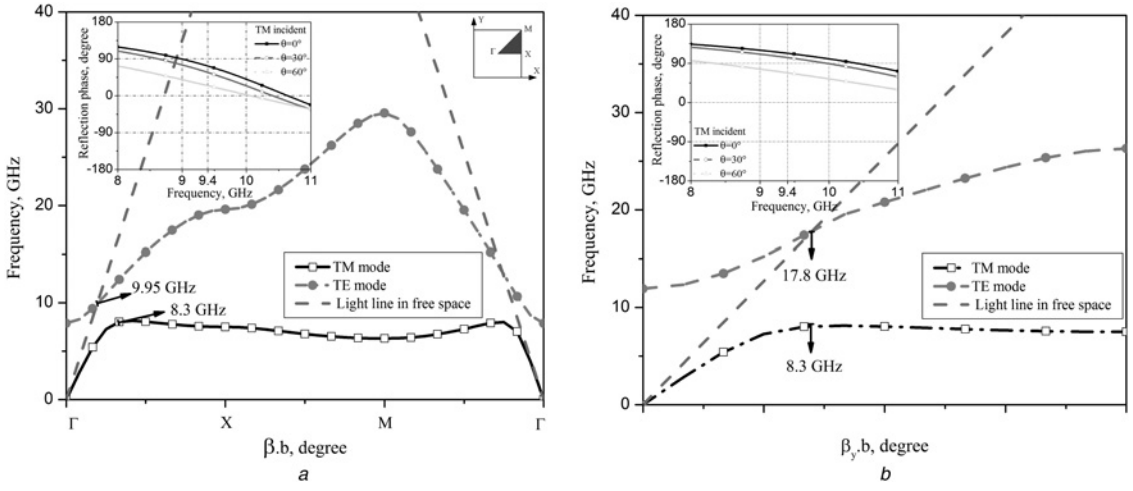

Fig. 9 *Simulated dispersion diagrams of EBG surfaces*

a Mushroom-EBG
b Soft-EBG

© The Institution of Engineering and Technology 2014

doi: 10.1049/iet-map.2014.0117

achieved in the antenna aperture, which considerably improves the gain of meta-based RQAA (by at least 2 dB) compared with the case composed only of metallic walls [26, 27]. This is basically because of the high impedance performance of meta-surfaces (see Fig. 9) for the propagating TM and TE waves in the desired operating band of 9–10 GHz. Therefore controlling the phase distribution in the aperture by using meta-surfaces in the *E*-plane is the reason of gain enhancement compared with the case where patch is surrounded by metallic fences. In addition, by examining the electric field at the edge of meta-surfaces in the aperture of the antenna made with soft-EBG, it can be observed that the orthogonal electric field almost tends to vanish, leading to a smaller back radiation in both *E* and *H* planes as summarised in Table 2.

3 Experimental results and discussion

To substantiate the results obtained, the two proposed RQAAs offering superior performances were fabricated and tested inside the anechoic chamber. A circle shaped patch with 3 mm radius centred at the feed location is removed from the ground plane during the fabrication process to accommodate the RF excitation port. Copper rivet is used as vias in the meta-surfaces. The outer and inner diameters of the rivets are 0.6 and 0.4 mm, respectively. Two pieces of copper plate with thickness of 0.5 mm were used as metallic fences in the *H*-plane of the RQAAs. Furthermore, some aluminium tape was utilised to connect the patch antenna to the metallic- and meta-walls. Fig. 10*a* demonstrates the photo of the fabricated RQAAs.

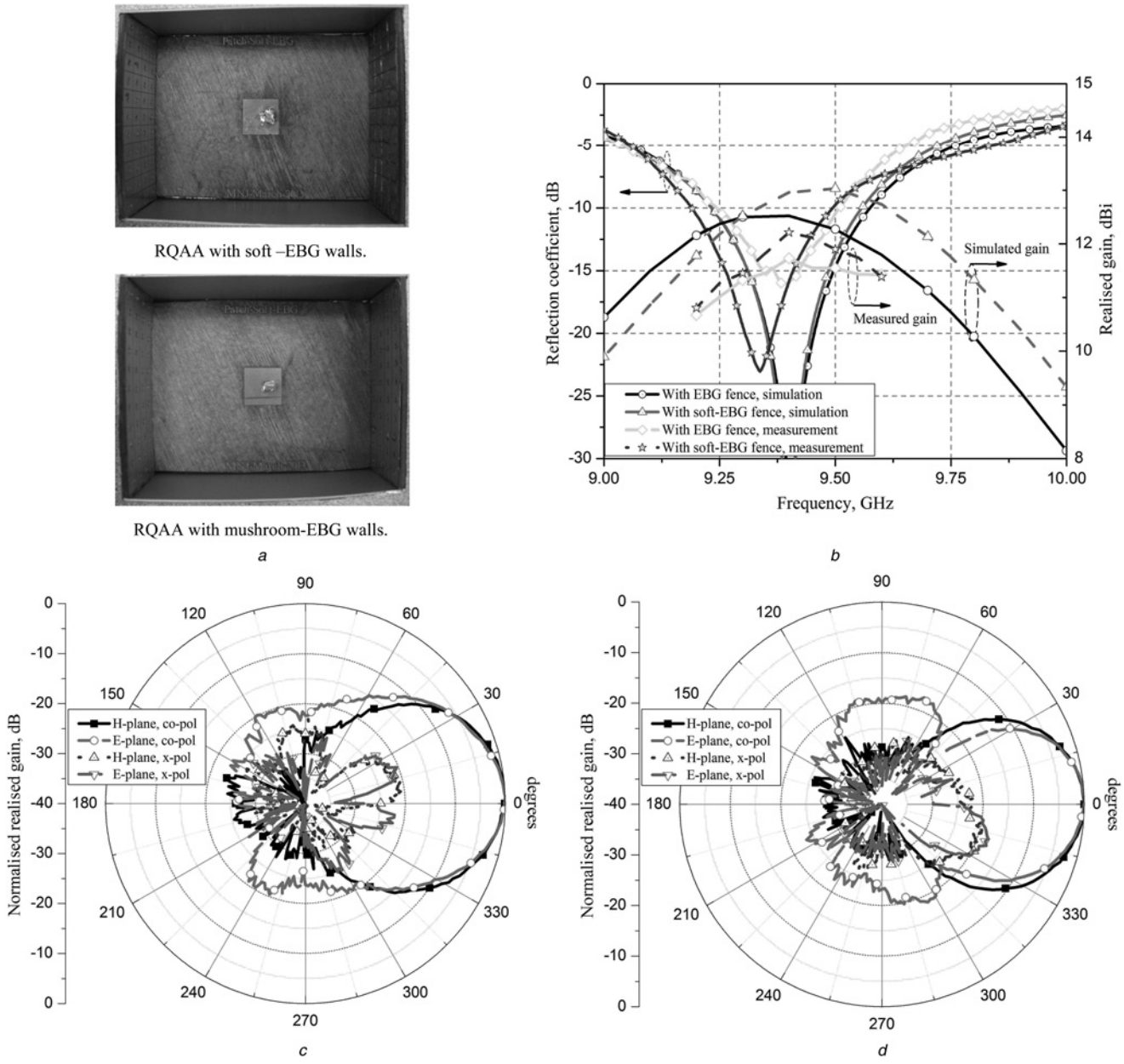

Fig. 10 *Photos of fabricated RQAAs and their radiation characteristics*

a Photo of fabricated RQAAs
b Simulated and measured reflection coefficients and realised gains of the fabricated RQAAs
c Radiation patterns of RQAA made with EBG fence
d Radiation patterns of RQAA made with soft-EBG fence

© The Institution of Engineering and Technology 2014

The measured reflection coefficients of the fabricated RQAAs are compared with the simulated ones as depicted in Fig. 10*b*. The investigation shows that since the sizes of the hole in the ground plane and also the SMA-connector modelled in the CST are slightly different than the sizes of the SMA-connector in practice, smaller matching bandwidths are obtained in the measurement compared with the simulations carried out for both antennas. Furthermore, some parts of this difference are also because of the out-centred position of the inner pin of the SMA-connector when it passes through the hole in the ground plane to be soldered to the patch. Since two similar SMAs have been used for the fabricated prototypes, obtaining a better bandwidth for one of them confirms this issue.

The measured realised gains of the antennas are compared with the simulated ones as demonstrated in Fig. 10*b*. Gain comparison method has been used to measure their gain in the broadside direction, that is, in the *Z*-direction, inside the anechoic chamber. The maximum realised gain for RQAA with EBG and soft-EBG walls are 11.73 and 12.2 dB, respectively, which are about 1 dB less than the simulated gains. The discrepancy between simulated and measured gains is probably because of the fabrication tolerance and measurement accuracy.

Comparing the obtained gains with that of a uniformly illuminated aperture with a physical area of A [15], the aperture efficiency of the antennas can be calculated by

$$\eta_{\text{ap}} = \frac{G\lambda_0^2}{4\pi A}$$

where λ_0 is the free space wavelength at 9.4 GHz, G is the realised gain of the antenna and A is the total size of the ground plane.

Summarised in Table 3, it is confirmed again that by using meta-surfaces the aperture efficiency of the patch antenna is significantly enhanced and RQAA made with soft meta-surface offers the maximum aperture efficiency.

Radiation patterns of the antennas were measured inside the anechoic chamber at the desired operating frequency 9.4 GHz. Figs. 10*c* and *d* demonstrate the measured co- and cross-polarised radiation patterns in the E and H planes. The characteristics of radiation patterns have been summarised in Table 2. The results of RQAA with EBG-fences demonstrate a symmetric radiation pattern with beam widths of 35.8 and 35.6° in E and H planes, respectively. The measured radiation pattern in the H-plane is slightly narrower than the one predicted by the simulation. The cross-polarisation is better than –20 dB in both E and H planes.

A notable difference between the measured and simulated cross-polarisations in the H-plane is observed, which is because of the ideal symmetric configuration of the antenna in the H-plane where the simulator predicts such low cross-polarisation exactly at $\varphi = 0°$. Back lobe levels are again in very good agreement in both planes with the predicted ones.

For the RQAA with soft-EBG fences, radiation performances almost similar to the RQAA with mushroom-EBGs were measured. However, two side lobes have been appeared in the E-plane radiation pattern which they considerably deviate the relevant back lobe level. The examination of the fabricated structure reveals that the size of aperture in the E-plane (i.e. distance between two EBG-walls) is slightly larger than the designed one (about 3 mm) because of the fences misalignment. This results in appearance of two side lobes from the sides of the E-plane radiation pattern.

4 Conclusion

The potentials of meta-surfaces constructed of mushroom-EBG structure as HIS and AMC in controlling the electromagnetic waves excited by a microstrip patch antenna are explored in planar and non-planar configurations. The results demonstrate that meta-surfaces with a length of maximum $\lambda_0/2$ (maximum four columns of unit cells) are adequate enough to obtain the desired radiation pattern in terms of gain, side/back lobe level in both planar and non-planar configurations. Indeed, by appropriately using these surfaces and controlling the propagating/incident electromagnetic waves, the gain of a simple patch antenna can be enhanced by more than 8 dB, indicating a notable improvement in its aperture efficiency, outperforming the optimum efficiency of a pyramidal horn antenna. As light weight, compact configurations with low side/back lobe levels and symmetric radiation patterns, these antennas can be good candidates as feeds for reflectors, which are constructed with planar technology.

5 References

1 Bhartia, P., Bahl, I., Garg, R., Ittipiboon, A.: 'Microstrip antenna design handbook' (Artech House, MA, USA, 2001)
2 David, M.P, Daniel, H.S.: 'Microstrip antennas: the analysis and design of microstrip antennas and arrays' (Wiley-IEEE Press, USA, 1995)
3 Imbriale, W.A., Gao, S., Boccia, L.: 'Space antenna handbook' (John Wiley & Sons Inc., New York, 2012)
4 Assailly, S., Terret, C., Daniel, J.P.: 'Some results on broad-band microstrip antenna with low cross polar and high gain', *IEEE Trans. Antennas Propag.*, 1991, **39**, (3), pp. 413–415
5 Lee, R.Q., Lee, K.F.: 'Gain enhancement of microstrip antennas with overlaying parasitic directors', *Electron. Lett.*, 1988, **24**, (11), pp. 656–658
6 Arnieri, E., Boccia, L., Amendola, G., Di Massa, G.: 'A compact high gain antenna for small satellite applications', *IEEE Trans. Antennas Propag.*, 2007, **55**, (2), pp. 277–282
7 Jackson, D.R., Alexopoulos, N.G.: 'Gain enhancement methods for printed circuit antennas', *IEEE Trans. Antennas Propag.*, 1985, **33**, (9), pp. 976–987
8 Yang, H., Alexopoulos, N.G.: 'Gain enhancement methods for printed circuit antennas through multiple superstrates', *IEEE Trans. Antennas Propag.*, 1987, **35**, (7), pp. 860–863
9 Leger, L., Monediere, T., Jecko, B.: 'Enhancement of gain and radiation bandwidth for a planar 1-D EBG antenna', *IEEE Microw. Wirel. Compon. Lett.*, 2005, **15**, (9), pp. 573–575
10 Gardelli, R., Albani, M., Capolino, F.: 'Array thinning by using antennas in a Fabry–Perot cavity for gain enhancement', *IEEE Trans. Antennas Propag.*, 2006, **54**, (7), pp. 1979–1990
11 Zhinong, Y., Kildal, P.S., Kishk, A.A.: 'Study of different realizations and calculation models for soft surfaces by using a vertical monopole on a soft disk as a test bed', *IEEE Trans. Antennas Propag.*, 1996, **44**, (11), pp. 1474–1481
12 Zhinong, Y., Kildal, P.S.: 'Improvements of dipole, helix, spiral, microstrip patch and aperture antennas with ground planes by using corrugated soft surfaces', *IEE Proc. Microw. Antennas Propag.*, 1996, **143**, (3), pp. 244–248
13 Sievenpiper, D., Zhang, L., Broas, R.F., Alexopolous, N.G., Yablonovitch, E.: 'High-impedance electromagnetic surfaces with a forbidden frequency band', *IEEE Trans. Microw. Theory Tech.*, 1999, **47**, (11), pp. 2059–2074
14 Goussetis, G., Feresidis, A.P., Vardaxoglou, J.C.: 'Tailoring the AMC and EBG characteristics of periodic metallic arrays printed on grounded dielectric substrate', *IEEE Trans. Antennas Propag.*, 2006, **54**, (1), pp. 82–89
15 Feresidis, A.P., Vardaxoglou, J.C.: 'High gain planar antenna using optimised partially reflective surfaces', *IEE Proc. Microw. Antennas Propag.*, 2001, **148**, (6), pp. 345–350

© The Institution of Engineering and Technology 2014

doi: 10.1049/iet-map.2014.0117

16 Yang, F., Rahmat-Samii, Y.: 'Microstrip antennas integrated with electromagnetic band-gap (EBG) structures: a low mutual coupling design for array applications', *IEEE Trans. Antennas Propag.*, 2003, **51**, (10), pp. 2936–2946
17 Foroozesh, A., Shafai, L.: 'Investigation into the application of artificial magnetic conductors to bandwidth broadening, gain enhancement and beam shaping of low profile and conventional monopole antennas', *IEEE Trans. Antennas Propag.*, 2011, **59**, (1), pp. 4–20
18 Engheta, N., Ziolkowski, R.W.: 'Metamaterials physics and engineering exploration' (John Wiley & Sons, Inc., NJ, USA, 2006)
19 Yang, F., Rahmat-Samii, Y.: 'Electromagnetic bandgap structures in antenna engineering' (Cambridge University Press, Cambridge, UK, 2008)
20 Lee, Y.J., Yeo, J., Mittra, R., Park, W.S.: 'Design of a high-directivity electromagnetic band gap (EBG) resonator antenna using a frequency-selective surface (FSS) superstrate', *Microw. Opt. Technol. Lett.*, 2004, **43**, (6), pp. 462–467
21 Foroozesh, A., Shafai, L.: 'Investigation into the effects of the patch-type FSS superstrate on the high-gain cavity resonance antenna design', *IEEE Trans. Antennas Propag.*, 2010, **58**, (2), pp. 258–270
22 Wang, S., Feresidis, A.P., Goussetis, G., Vardaxoglou, J.C.: 'High-gain subwavelength resonant cavity antennas based on metamaterial ground planes', *IEE Proc. Microw. Antennas Propag.*, 2006, **153**, (1), pp. 1–6
23 Foroozesh, A., Shafai, L.: 'Application of combined electric- and magnetic-conductor ground planes for antenna performance enhancement', *Can. J. Electr. Comput. Eng.*, 2008, **33**, (2), pp. 87–98
24 Yang, F., Coccioli, R., Qian, Y., Itoh, T.: 'PBG-assisted gain enhancement of patch antennas on high-dielectric constant substrate', *IEEE Int. Symp. Antennas Propag. Soc.*, 1999, **3**, pp. 1920–1923
25 Lee, Y.J., Yeo, J., Ko, K.D., Mittra, R., Lee, Y., Park, W.S.: 'A novel design technique for control of defect frequencies of an electromagnetic bandgap (EBG) superstrate for dual-band directivity enhancement', *Microw. Opt. Technol. Lett.*, 2004, **42**, (1), pp. 25–31
26 Kildal, P.S., Lier, E.: 'Hard horns improve cluster feeds of satellite antennas', *Electron. Lett.*, 1988, **24**, (8), pp. 491–492
27 Lier, E., Kildal, P.S.: 'Soft and hard horn antennas', *IEEE Trans. Antennas Propag.*, 1988, **36**, (8), pp. 1152–1157
28 Kildal, P.S.: 'Definition of artificially soft and hard surfaces for electromagnetic waves', *Electron. Lett.*, 1988, **24**, (3), pp. 168–170
29 Lier, E., Pettersen, T.S.: 'The strip-loaded hybrid-mode feed horn', *IEEE Trans. Antennas Propag.*, 1987, **35**, (9), pp. 1086–1089
30 Lier, E.: 'Review of soft and hard horn antennas, including metamaterial-based hybrid-mode horns', *IEEE Mag. Antennas Propag.*, 2010, **52**, (2), pp. 31–39
31 Yakovlev, A.B., Silveirinha, M.G., Luukkonen, O., Simovski, C.R., Nefedov, I.S., Tretyakov, S.A.: 'Characterization of surface-wave and leaky-wave propagation on wire-medium slabs and mushroom structures based on local and nonlocal homogenization models', *IEEE Trans. Microw. Theory Tech.*, 2009, **57**, (11), pp. 2700–2714
32 Stutzman, W.L., Thiele, G.A.: 'Antenna theory and design' (John Wiley & Sons Inc., USA, 2012, 3rd edn.)

© The Institution of Engineering and Technology 2014

Copyright of IET Microwaves, Antennas & Propagation is the property of Institution of Engineering & Technology and its content may not be copied or emailed to multiple sites or posted to a listserv without the copyright holder's express written permission. However, users may print, download, or email articles for individual use.